arXiv:2004.00374v1 [cond-mat.mes-hall] 1 Apr 2020

Majorana molecules and their spectral fingerprints

J. E. Sanches[1], L. S. Ricco[1], W. N. Mizobata[1], Y. Marques[2], M. de Souza[3], I. A. Shelykh[2,4] and A. C. Seridonio[1,3]
[1]*Departamento de Física e Química, Unesp - Univ Estadual Paulista, 15385-000, Ilha Solteira, SP, Brazil*
[2]*ITMO University, St. Petersburg 197101, Russia*
[3]*IGCE, Unesp - Univ Estadual Paulista, Departamento de Física, 13506-900, Rio Claro, SP, Brazil*
[4]*Science Institute, University of Iceland, Dunhagi 3, IS-107, Reykjavik, Iceland*

We introduce the concept of a Majorana molecule, a topological bound state appearing in the geometry of a double quantum dot (QD) structure flanking a topological superconducting nanowire. We demonstrate that, if Majorana bound states (MBSs) at opposite edges are probed nonlocally in a two probe experiment, the spectral density of the system reveals the so-called *half-bowtie* profiles, while Andreev bound states (ABSs) become resolved into bonding and antibonding molecular configurations. We reveal that this effect is due to the Fano interference between singlet and triplet *pseudospin* pairing channels and propose a protocol for the experimental detection of the predicted effects.

Introduction.— The recent decade witnessed the increasing interest of the condensed matter community in Majorana physics. In particular, the concept of Majorana bound states (MBSs) as promising building blocks for topologically protected and fault-tolerant quantum computing received special attention [1–6]. MBSs are zero-modes appearing at topological boundaries of condensed matter systems with spinless p-wave superconductivity, as it was first predicted by A. Y. Kitaev in his seminal work [7]. They manifest themselves via zero-bias peak (ZBP) signature in local conductance measurements [8]. As candidates for hosting nonlocal MBSs, such material platforms as ferromagnetic atomic chains [9–19] and semiconductor hybrid nanowires [8, 20–24] were proposed. Isolated MBSs are also supposed to be attached to cores of superconducting vortices[25, 26].

In this work, we propose the concept of a Majorana molecule. It appears in the configuration similar to those considered in the end of Ref. [23] and schematically shown in Fig.1(a) of the current paper. It consists of a one-dimensional (1D) topological superconductor (TSC) hosting MBSs at the edges, which hybridize with normal fermionic states of a pair of quantum dots (QDs) flanking the TSC wire, placed in the strong longitudinal magnetic field. If the latter is strong enough, so that Zeeman splitting becomes much larger than all other characteristic energies of the system, the *spinless* condition is fulfilled. In this case, the tuning of the parameters of the system leads to a crossover between the well-known regime of individual Andreev bound states (ABSs) [23] (*The Majorana molecule turned-off*), and the regime in which one witnesses the splitting of the ABS into bonding and antibonding molecular configurations (*The Majorana molecule turned-on*). The formation of these states can be described in terms of the so-called *pseudospins* ($\uparrow,\downarrow$), which determine the structure of the QDs orbitals by means of superconducting singlet and triplet states. Note that, contrary to the single QD geometry considered before [23, 24], in our setup the QDs act as a nonlocal two-probe detector which catches the Fano interference effects [27, 28] between various tunneling paths, including those involving the MBSs. This can result in plethora of intriguing transport signatures [29–38], such as so-called *Majorana oscillations* [38]. We demonstrate that, similar to what happens in the system of a pair of QDs placed within a semiconductor [39] or a Dirac-Weyl semimetal host [40, 41], the Fano effect in the considered system defines the novel type of molecular binding of QD orbitals, and leads to the formation of a Majorana molecule, characterized by the so-called *half-bowtie* profiles in the spectral density of states.

The Model.—The geometry we consider is shown in the Fig.1(a). The system under study consists of a 1D-TSC nanowire with nonlocal MBSs formed at its edges and flanked by a pair of QDs. The latter are attached to metallic leads, serving as source and drain of an electric current through the system. We suggest that the external magnetic field applied along the direction of the wire is large enough, so that only spin up states lie below the Fermi energy, and spin down states can be just totally excluded from the consideration [42–44]. We account for the possible coupling between MBSs localized at the opposite edges of the TSC wire, which can change their nonlocality degree and lead to the crossover between highly nonlocal MBSs and more local ABSs.

The Hamiltonian of the system reads:

$$\begin{aligned}\mathcal{H} &= \sum_{\alpha\mathbf{k}} \varepsilon_{\mathbf{k}} \tilde{c}^{\dagger}_{\alpha\mathbf{k}} \tilde{c}_{\alpha\mathbf{k}} + \sum_{\alpha} \tilde{\varepsilon}_{\alpha} \tilde{d}^{\dagger}_{\alpha} \tilde{d}_{\alpha} + t_{\mathrm{c}}(\tilde{d}^{\dagger}_{L}\tilde{d}_{R} + \mathrm{H.c.}) \\ &+ \mathcal{V}\sum_{\alpha\mathbf{k}}(\tilde{c}^{\dagger}_{\alpha\mathbf{k}}\tilde{d}_{\alpha} + \mathrm{H.c.}) + \lambda_{L1}(\tilde{d}_{L} - \tilde{d}^{\dagger}_{L})\Psi_1 \\ &+ i\lambda_{L2}(\tilde{d}_{L} + \tilde{d}^{\dagger}_{L})\Psi_2 + i\lambda_{R1}(\tilde{d}_{R} + \tilde{d}^{\dagger}_{R})\Psi_2 \\ &+ \lambda_{R2}(\tilde{d}_{R} - \tilde{d}^{\dagger}_{R})\Psi_1 + i\varepsilon_M \Psi_1\Psi_2, \end{aligned} \tag{1}$$

where the operators $c^{\dagger}_{\alpha\mathbf{k}}, c_{\alpha\mathbf{k}}$ correspond to electrons in the right and left metallic leads $\alpha = L, R$ having momentum $\mathbf{k}$ and energy $\varepsilon_{\mathbf{k}}$. The operators $\tilde{d}^{\dagger}_{\alpha}, \tilde{d}_{\alpha}$ describe the localized orbitals in the right and left QDs with energies $\tilde{\varepsilon}_{\alpha}$, t_{c} is the hopping term corresponding to the normal direct tunneling between the QDs, which can lead to the formation of usual molecular orbitals [39] and $\mathcal{V}$ describes the strength of the coupling between the QDs and the leads (we take it equal for right and left QDs). At the edges of the TSC wire, the nonlocal MBSs described by the operators $\Psi_j = \Psi_j^\dagger$, couple to the QDs with the amplitudes $\lambda_{\alpha j}$ with $j = 1, 2$ (the ratio $\eta_\alpha = |\lambda_{\alpha 1}/\lambda_{\alpha 2}|$ defines the nonlocality degree) and to each other via the overlap term ε_M.

Linear combination of the Majorana operators

$$f_\uparrow = \frac{1}{\sqrt{2}}(\Psi_1 + i\Psi_2) \tag{2}$$

forms a regular fermionic state. Performing the rotation in the *pseudospin* space $\sigma = \pm 1$ ($\uparrow, \downarrow$), corresponding to R and L states, $\tilde{d}_L = \cos\theta d_\uparrow - \sin\theta d_\downarrow$, $\tilde{d}_R = \sin\theta d_\uparrow + \cos\theta d_\downarrow$, $\tilde{c}_{\mathbf{k}L} = \cos\theta c_{\mathbf{k}\uparrow} - \sin\theta c_{\mathbf{k}\downarrow}$, $\tilde{c}_{\mathbf{k}R} = \sin\theta c_{\mathbf{k}\uparrow} + \cos\theta c_{\mathbf{k}\downarrow}$ with $\cos(2\theta) = -\frac{\triangle\varepsilon}{\sqrt{4(t_c)^2 + (\triangle\varepsilon)^2}}$ and $\triangle\varepsilon = \tilde{\varepsilon}_L - \tilde{\varepsilon}_R$, the Hamiltonian of the system can be rewritten as:

$$\mathcal{H} = \sum_{\mathbf{k}\sigma} \varepsilon_{\mathbf{k}} c_{\mathbf{k}\sigma}^\dagger c_{\mathbf{k}\sigma} + \sum_\sigma \varepsilon_{d\sigma} d_\sigma^\dagger d_\sigma + \mathcal{V} \sum_{\mathbf{k}\sigma} (c_{\mathbf{k}\sigma}^\dagger d_\sigma + \text{H.c.}) + \varepsilon_M (f_\uparrow^\dagger f_\uparrow - \frac{1}{2}) + \sum_\sigma (\mathcal{V}_\sigma^- d_\sigma f_\uparrow^\dagger + \mathcal{V}_\sigma^+ d_\sigma f_\uparrow + \text{H.c.}), \tag{3}$$

where $\varepsilon_{d\sigma} = \frac{(\tilde{\varepsilon}_L + \tilde{\varepsilon}_R)}{2} - \frac{\sigma}{2}\sqrt{4(t_c)^2 + (\triangle\varepsilon)^2}$, $\mathcal{V}_\uparrow^\mp = \frac{1}{\sqrt{2}}[(\lambda_{R2} \mp \lambda_{R1})\sin\theta + (\lambda_{L1} \mp \lambda_{L2})\cos\theta]$ and $\mathcal{V}_\downarrow^\mp = \frac{1}{\sqrt{2}}[(\lambda_{R2} \mp \lambda_{R1})\cos\theta - (\lambda_{L1} \mp \lambda_{L2})\sin\theta]$.

The Hamiltonian given in Eq. (3) corresponds to the mapping of the original problem to one equivalent to a single spinor QD coupled to fermionic state $f_\uparrow$ and characterized by a mixture of superconducting states, having p and s-wave symmetries. The amplitudes $\mathcal{V}_\uparrow^+$ and $\mathcal{V}_\downarrow^+$ correspond to the formation of Cooper pairs in triplet ($d_\uparrow f_\uparrow$) and singlet ($d_\downarrow f_\uparrow$) configurations, while the terms $\mathcal{V}_{\uparrow(\downarrow)}^-$ give the normal coupling between the QD and $f_\uparrow$ with either spin conservation ($\mathcal{V}_\uparrow^-$) or spin flip ($\mathcal{V}_\downarrow^-$). The sketch of the equivalent geometry is depicted in Fig.1(b).

In the following discussion, we will consider the case of the identical QDs, corresponding to $\tilde{\varepsilon}_L = \tilde{\varepsilon}_R = \varepsilon_d$ and $\theta = \frac{\pi}{4}$. The QD states corresponding to the opposite pseudospins are now simply symmetric and antisymmetric combinations between the orbitals of right and left QDs:

$$d_\uparrow = \frac{\tilde{d}_R + \tilde{d}_L}{\sqrt{2}} \text{ and } d_\downarrow = \frac{\tilde{d}_R - \tilde{d}_L}{\sqrt{2}}, \tag{4}$$

which represent the bonding and antibonding molecular states with the energies $\varepsilon_{d\sigma} = \varepsilon_d - \sigma t_c$, respectively. Moreover,

$$\mathcal{V}_\uparrow^\mp = \frac{\lambda_{R2} + \lambda_{L1} \mp (\lambda_{R1} + \lambda_{L2})}{2} \tag{5}$$

and

$$\mathcal{V}_\downarrow^\mp = \frac{\lambda_{R2} - \lambda_{L1} \mp (\lambda_{R1} - \lambda_{L2})}{2}. \tag{6}$$

As we are interested in the pairing mediated by MBSs only, we put $t_c = 0$. As we will see, the communication between the QDs lead to the splitting of the ABSs into ABS-$\uparrow$ and ABS-$\downarrow$, and formation of a Majorana molecule.

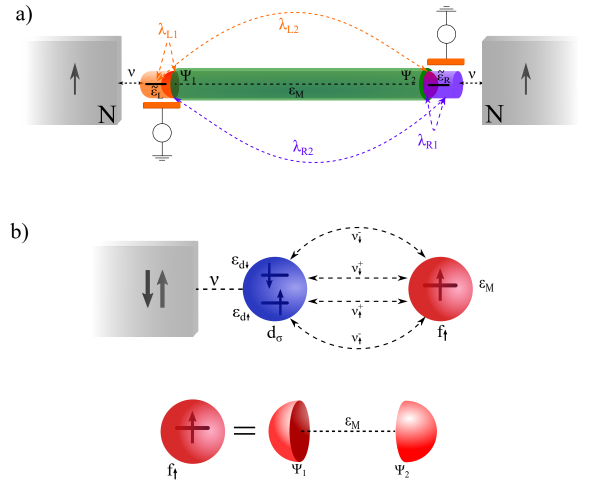

Figure 1. (Color online) (a) The sketch of the considered system with one-dimensional topological superconductor (1D-TSC) and nonlocal Majorana bound states (MBSs) $\Psi_j = \Psi_j^\dagger$ ($j = 1, 2$) at the edges and flanked by a pair of QDs with energies $\tilde{\varepsilon}_L$ and $\tilde{\varepsilon}_R$ coupled to metallic leads, via the hybridization $\mathcal{V}$. The nonlocal MBSs couple to the QDs via the amplitudes $\lambda_{\alpha j}$ ($\alpha = L, R$) and to each other by the overlap term ε_M. The system is characterized by *spinless* and p-wave superconductivity in spin up ($\uparrow$) channel, due to the large Zeeman splitting. (b) Mapping of the original system into equivalent geometry with a single QD with *pseudospin* degree of freedom. The amplitudes $\mathcal{V}_\uparrow^+$ and $\mathcal{V}_\downarrow^+$ refer to triplet ($d_\uparrow f_\uparrow$) and singlet ($d_\downarrow f_\uparrow$) channels of the formation of Cooper pairs spatially split into the orbitals with energies $\varepsilon_{d\sigma}$ and ε_M. The terms $\mathcal{V}_\uparrow^-$ and $\mathcal{V}_\downarrow^-$ stand for *pseudospin* ballistic and spin flip transport processes through such orbitals, respectively. The nonlocal orbital $f_\uparrow$ is formed by a pair of the MBSs.

We characterize the QDs by their normalized spectral densities

$$\tau_{jl}(\omega) = -\Gamma \text{Im}(\langle\langle d_j; d_l^\dagger \rangle\rangle), \tag{7}$$

where $j, l = L, R$, $\langle\langle d_j; d_l^\dagger \rangle\rangle$ are retarded Green's functions (GFs) in the frequency domain and $\Gamma = \pi\mathcal{V}^2 \sum_{\mathbf{k}} \delta(\varepsilon - \varepsilon_{\mathbf{k}})$ [45]. Performing the pseudospin rotation given by Eq. (4), we get

$$\tau_{LL(RR)}(\omega) = \frac{1}{2}\{(\tau_{\uparrow\uparrow} + \tau_{\downarrow\downarrow}) \mp (\tau_{\uparrow\downarrow} + \tau_{\downarrow\uparrow})\} \tag{8}$$

and

$$\tau_{RL(LR)}(\omega) = \frac{1}{2}\{(\tau_{\uparrow\uparrow} - \tau_{\downarrow\downarrow}) \mp (\tau_{\uparrow\downarrow} - \tau_{\downarrow\uparrow})\} \tag{9}$$

for the local and nonlocal QDs densities, respectively. The presence of the terms $\tau_{\uparrow\downarrow}(\tau_{\downarrow\uparrow})$ accounts for the Fano interference in the *pseudospin* channels. Conversely, the QDs $\tilde{d}_L$ and $\tilde{d}_R$ interfere to each other, thus forming $\tau_{\uparrow\uparrow}(\omega)$ (bonding) and $\tau_{\downarrow\downarrow}(\omega)$ (antibonding) orbitals

$$\tau_{\uparrow\uparrow(\downarrow\downarrow)}(\omega) = \frac{1}{2}\{(\tau_{LL} + \tau_{RR}) \pm (\tau_{RL} + \tau_{LR})\} \tag{10}$$

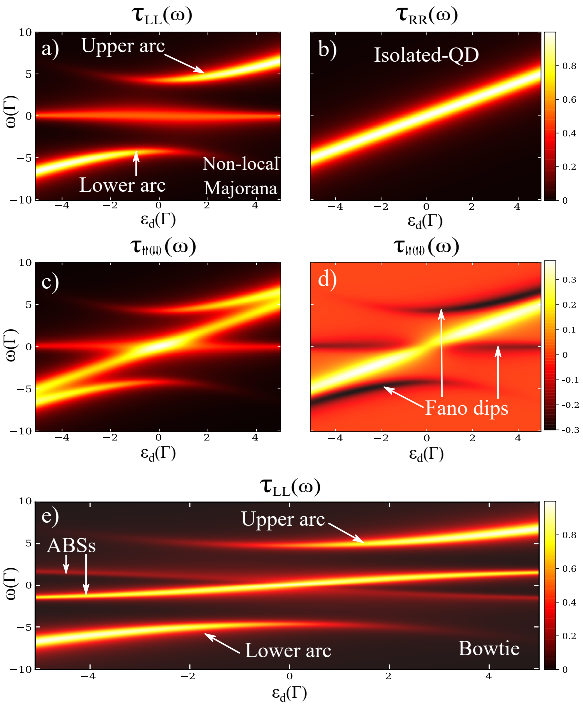

Figure 2. (Color online) *The Majorana molecule turned-off scenario.* Color maps of the spectral density of the QDs spanned by ω and $\varepsilon_d = \tilde{\varepsilon}_L = \tilde{\varepsilon}_R$. Panels (a)-(d) correspond to the case of a right QD decoupled from MBSs, $\lambda_{L1} = 3\Gamma$ and $\lambda_{L2} = \lambda_{R1} = \lambda_{R2} = \varepsilon_M = 0$. In panel (a) the density plot of $\tau_{LL}(\omega)$ demonstrates clearly visible horizontal bright line, corresponding to the ZBP due to the coupling with the MBS Ψ_1, which is robust against changes in ε_d [43]. In panel (b) the spectral density $\tau_{RR}(\omega)$ reveals solely the resonant level of the right QD, uncoupled to MBSs at $\omega = \varepsilon_d$. In this regime, Fano interference between the QDs is absent and $\tau_{RL}(\omega) = \tau_{LR}(\omega) = 0$. Panels (c) and (d) show $\tau_{\uparrow\uparrow}(\omega) = \tau_{\downarrow\downarrow}(\omega)$, and $\tau_{\uparrow\downarrow}(\omega) = \tau_{\downarrow\uparrow}(\omega)$ respectively, which reveal clear signatures of constructive and destructive Fano interference. Panel (e) accounts for the coupling of the left QD to the overlapping MBSs ($\lambda_{L1} = 3\Gamma$, $\lambda_{L2} = 0.001\Gamma$, $\lambda_{R1} = \lambda_{R2} = 0$ and $\varepsilon_M = 2\Gamma$). In this case the density plot for τ_{LL} reveals the transformation of the horizontal bright line, corresponding to the ZBP, into a *bowtie* profile, characteristic for split ABSs [23].

and

$$\tau_{\uparrow\downarrow(\downarrow\uparrow)}(\omega) = \frac{1}{2}\{(\tau_{RR} - \tau_{LL}) \pm (\tau_{LR} - \tau_{RL})\}. \quad (11)$$

To evaluate $\langle\langle d_\sigma; d^\dagger_{\sigma'}\rangle\rangle$, we apply the equation-of-motion method[46] to Eq.(3), which gives:

$$(\omega + i0^+)\langle\langle d_\sigma; d^\dagger_{\sigma'}\rangle\rangle = \delta_{\sigma\sigma'} + \langle\langle [d_\sigma, \mathcal{H}]\,; d^\dagger_{\sigma'}\rangle\rangle. \quad (12)$$

The last term in the Eq.(12) will generate the anomalous Green functions $\langle\langle d^\dagger_\sigma; d^\dagger_{\sigma'}\rangle\rangle$. As the Hamiltonian is quadratic, the system of equations can be closed and written in the matrix form as

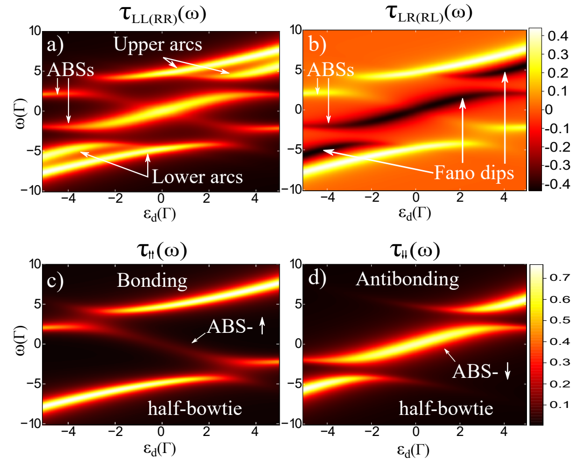

Figure 3. (Color online) *The Majorana molecule turned-on scenario.* Color maps of the spectral density of the QDs spanned by ω and $\varepsilon_d = \tilde{\varepsilon}_L = \tilde{\varepsilon}_R$. The parameters of the system are $\lambda_{L1} = \lambda_{R1} = 3\Gamma$, $\lambda_{L2} = \lambda_{R2} = 1.5\Gamma$ and $\varepsilon_M = 0.05\Gamma$. Panel (a) shows the profiles of $\tau_{LL}(\omega) = \tau_{RR}(\omega)$, and reveals the splitting of the upper and lower arcs due to the formation of the bonding (ABS-↑) and antibonding (ABS-↓) Andreev molecular states. The *pseudospin* lifting in $\tau_{\uparrow\uparrow(\downarrow\downarrow)}(\omega)$ is attributed to the Fano interference between $\tau_{LL(RR)}(\omega)$ and $\tau_{LR(RL)}(\omega)$, which appears in panel (b). Formation of the aforementioned molecular states is even more clearly visible in the panels (c) and (d), corresponding to $\tau_{\uparrow\uparrow}(\omega)$ and $\tau_{\downarrow\downarrow}(\omega)$, where at the novel *half-bowtie*-like structures are formed. In this regime $\tau_{\uparrow\downarrow}(\omega) = \tau_{\uparrow\downarrow}(\omega) = 0$, and Majorana molecular states are resolved in the *pseudospin* basis.

$\boldsymbol{A}^\sigma(\omega)\,(\,\langle\langle d_\sigma; d^\dagger_\sigma\rangle\rangle \;\; \langle\langle d_{\bar\sigma}; d^\dagger_\sigma\rangle\rangle \;\; \langle\langle d^\dagger_\sigma; d^\dagger_\sigma\rangle\rangle \;\; \langle\langle d^\dagger_{\bar\sigma}; d^\dagger_\sigma\rangle\rangle)^T = (1 \;\; 0 \;\; 0 \;\; 0\,)^T$, with

$$\boldsymbol{A}^\sigma(\omega) = \begin{bmatrix} a_\sigma(\omega) & -k^{\sigma\bar\sigma}_{2-}(\omega) & k^{\sigma\sigma}_{1-}(\omega) & k^{\sigma\bar\sigma}_{1-}(\omega) \\ -k^{\bar\sigma\sigma}_{2-}(\omega) & a_{\bar\sigma}(\omega) & k^{\bar\sigma\sigma}_{1-}(\omega) & k^{\bar\sigma\bar\sigma}_{1-}(\omega) \\ k^{\sigma\sigma}_{1+}(\omega) & k^{\sigma\bar\sigma}_{1+}(\omega) & b_\sigma(\omega) & -k^{\sigma\bar\sigma}_{2+}(\omega) \\ k^{\bar\sigma\sigma}_{1+}(\omega) & k^{\bar\sigma\bar\sigma}_{1+}(\omega) & -k^{\bar\sigma\sigma}_{2+}(\omega) & b_{\bar\sigma}(\omega) \end{bmatrix}, \quad (13)$$

where $\bar\sigma = -\sigma$, $k^{\sigma\sigma'}_{1\mp}(\omega) = \mathcal{V}^-_\sigma\mathcal{V}^+_{\sigma'}(\omega\mp\varepsilon_M)^{-1} + \mathcal{V}^-_{\sigma'}\mathcal{V}^+_\sigma(\omega\pm\varepsilon_M)^{-1}$, $k^{\sigma\sigma'}_{2\mp}(\omega) = \mathcal{V}^-_\sigma\mathcal{V}^-_{\sigma'}(\omega\mp\varepsilon_M)^{-1} + \mathcal{V}^+_\sigma\mathcal{V}^+_{\sigma'}(\omega\pm\varepsilon_M)^{-1}$, $a_\sigma(\omega) = \omega - \varepsilon_{d\sigma} - k^{\sigma\sigma}_{2-} + i\Gamma$ and $b_\sigma(\omega) = \omega + \varepsilon_{d\sigma} - k^{\sigma\sigma}_{2+} + i\Gamma$.

Results and Discussion.—We assume the temperature $T = 0$K and put $\Gamma = 40\mu eV$ [43] as the energy scale of the model parameters of the system. Our aim is to investigate the spectral function of the considered system defined by the Eq. (7).

To better understand the situation qualitatively, we start from the geometry wherein only the left QD is coupled to MBSs, *i.e,* from the Majorana molecule turned-off scenario. We present the results for both the case of isolated highly nonlocal MBS [43] (Fig.2(a)) and the case of overlapping MBSs (Fig.2(e)). For both cases we present the 2D plots of the spectral functions in the ω and ε_d axes.

Fig.2(a) shows the spectral function corresponding to the left QD, $\tau_{LL}(\omega)$ in the situation, when it is coupled only to the closest MBS ($\lambda_{L1} = 3\Gamma$ and $\lambda_{R1} = \lambda_{R2} = \lambda_{L2} = \varepsilon_M = 0$). In perfect agreement with the Ref.[43], one can see the bright plateau at $\omega = 0$, corresponding to the ZBP in the conductance, which is robust against the ε_d perturbations and is provided by the presence of highly nonlocal MBSs. The upper and lower arcs correspond to the QD states split by the coupling to the MBS Ψ_1. Naturally, as right QD is decoupled from both MBSs, its spectral function $\tau_{RR}(\omega)$, shown in the Fig.2(b) is trivial and consists of a single peak corresponding to $\omega = \varepsilon_d$. As the QDs do not communicate through the 1D-TSC, $\tau_{RL}(\omega) = \tau_{LR}(\omega) = 0$.

In the *pseudospin* basis, the latter condition, according to the Eqs.(5,6,10,11), imposes the *pseudospin* degeneracy, so that $\tau_{\uparrow\uparrow}(\omega) = \tau_{\downarrow\downarrow}(\omega)$ (shown in the Fig.2(c)), and $\tau_{\downarrow\uparrow}(\omega) = \tau_{\uparrow\downarrow}(\omega)$ (Fig.2(d)), $|\mathcal{V}_\uparrow^-| = |\mathcal{V}_\downarrow^-|$ and $|\mathcal{V}_\uparrow^+| = |\mathcal{V}_\downarrow^+|$, and, besides, $|\mathcal{V}_\sigma^-| = |\mathcal{V}_\sigma^+|$. *Pseudospin* degeneracy, in particular, means, that singlet and triplet Cooper pairing contribute to the Hamiltonian on the equal footing. The fact, that $\tau_{\downarrow\uparrow(\uparrow\downarrow)}(\omega) \neq 0$ means, that two *pseudospin* channels, corresponding to bonding and antibonding states, are non-orthogonal, and thus Majorana molecule is not formed. Spectral functions in the *pseudospin* basis are presented in the Figs.2(c)-(d), and reveal clear signatures of the Fano interference peaks and dips.

If one accounts for the coupling of the left QD to the MBS Ψ_2 ($\lambda_{L2} = 0.001\Gamma$), with finite overlap between the states Ψ_1 and Ψ_2 ($\varepsilon_M = 2\Gamma$), but keeps right QD decoupled ($\lambda_{R1} = \lambda_{R2} = 0$), the spectral function $\tau_{LL}(\omega)$ reveals characteristic bowtie profile [23, 24] (also referred as double fork [44]) instead of a robust ZBP. This corresponds to the presence in the system of a pair of trivial ABSs, as it is shown in the Fig.2(e). Other spectral functions remain qualitatively the same. The condition of *pseudospin* degeneracy still holds and a Majorana molecule is not formed.

Now, we can consider the symmetric case sketched in Fig.1(a) with $\lambda_{L1} = \lambda_{R1} = 3\Gamma$, $\lambda_{L2} = \lambda_{R2} = 1.5\Gamma$ and $\varepsilon_M = 0.05\Gamma$, corresponding to *The Majorana molecule turned-on scenario*: both QDs are coupled to both MBSs, and thus interfere with each other through the 1D-TSC. In this situation, a *bowtie*-like signature emerges in the spectral density $\tau_{LL(RR)}(\omega)$, as it can be seen from Fig. 3(a). Moreover, the features characteristic to usual molecular binding can be seen, as upper and lower arcs provided by the coupling of the QD states, visible in Fig. 2(e), become split in Fig. 3(a) due to the TSC-mediated overlap of the states of right and left QDs. Naturally, this leads to $\tau_{RL}(\omega) = \tau_{LR}(\omega) \neq 0$ (see Fig. 3(b)), which, according to the Eqs. (10) and (11) means that $\tau_{\uparrow\uparrow}(\omega) \neq \tau_{\downarrow\downarrow}$ and $\tau_{\downarrow\uparrow(\uparrow\downarrow)}(\omega) = 0$.

Physically, this means that spin up and spin down channels become decoupled in the *pseudospin* basis and a Majorana molecule, which is a bonding or antibonding superposition of ABSs is formed. The latter manifest themselves in the spectral profiles of $\tau_{\uparrow\uparrow}(\omega)$ and $\tau_{\downarrow\downarrow}(\omega)$ shown in Figs.3(c) and (d), respectively as *half-bowtie* signatures. They are consequences of the Fano interference between $\tau_{LR}(\omega)$ and $\tau_{RL}(\omega)$, shown in Fig.3(b). Note that the latter contains both peaks and pronounced Fano dips, which interfere constructively or destructively depending on the sign in the Eqs. (10) and (11), with the peaks in the spectral densities of $\tau_{LL}(\omega)$ and $\tau_{RR}(\omega)$, which gives in the end the mentioned *half-bowtie* profiles.

In terms of the effective Hamiltonian (Eq. 3), the considered regime corresponds to the case, when $|\mathcal{V}_\downarrow^-| \neq 0$, $|\mathcal{V}_\uparrow^-| = 0$, $|\mathcal{V}_\downarrow^+| = 0$ and $|\mathcal{V}_\uparrow^+| \neq 0$. This means that only triplet-type Cooper pairing ($|\mathcal{V}_\uparrow^+| \neq 0$) and normal electron tunneling with spin flip ($|\mathcal{V}_\downarrow^-| \neq 0$) contribute to the transport assisted by the formation of Majorana molecules.

Conclusions.—In summary, we have proposed the concept of a Majorana molecule, a bonding or antibonding state appearing in the system of a pair of QDs flanking a 1D-TSC nanowire. The coupling between QDs is achieved via the channel provided by the presence of MBSs. It is demonstrated that these states manifest themselves via *half-bowtie* spectral fingerprints in the spectral density of states, which are qualitatively different from full *bowtie* profiles, characteristic to the case of a single QD.

Acknowledgments.—We thank the Brazilian funding agencies CNPq (Grants No. 305668/2018-8 and No. 302498/2017-6), the São Paulo Research Foundation (FAPESP; Grant No. 2015/23539-8) and Coordenação de Aperfeiçoamento de Pessoal de Nível Superior – Brasil (CAPES) – Finance Code 001. Y.M. and I.A.S. acknowledge support from the Government of the Russian Federation through the Megagrant 14.Y26.31.0015, and ITMO 5-100 Program.

[1] R. Aguado, Riv. Nuovo Cimento 40, 523 (2017).
[2] C. Nayak, S. H. Simon, A. Stern, M. Freedman, and S. Das Sarma, Rev. Mod. Phys. 80, 1083 (2008).
[3] J. Alicea, Rep. Prog. Phys. 75, 076501 (2012).
[4] S. R. Elliott and M. Franz, Rev. Mod. Phys. 87, 137 (2015).
[5] G. Goldstein and C. Chamon, Phys. Rev. B 84, 205109 (2011).
[6] J. C. Budich, S. Walter, and B. Trauzettel, Phys. Rev. B 85, 121405(R) (2012).
[7] A. Y. Kitaev, Phys. Usp. 44, 131 (2001).
[8] H. Zhang, C.-X. Liu, S. Gazibegovic, D. Xu, J. A. Logan, G. Wang, N. van Loo, J. D. S. Bommer, M. W. A. de Moor, D. Car, R. L. M. Op het Veld, P. J. van Veldhoven, S. Koelling, M. A. Verheijen, M. Pendharkar, D. J. Pennachio, B. Shojaei, J. S. Lee, C. J. Palmstrom, E. P. A. M. Bakkers, S. D. Sarma, and L. P. Kouwenhoven, Nature (London) 556, 74 (2018).

[9] T.-P. Choy, J.M. Edge, A.R. Akhmerov, C.W.J. Beenakker, Phys. Rev. B 84, 195442 (2011).
[10] S. Nadj-Perge, I.K. Drozdov, B.A. Bernevig, A. Yazdani, Phys. Rev. B 88, 020407 (2013).
[11] J. Klinovaja, P. Stano, A. Yazdani, D. Loss, Phys. Rev. Lett. 111, 186805 (2013).
[12] B. Braunecker, P. Simon, Phys. Rev. Lett. 111, 147202 (2013).
[13] M.M. Vazifeh, M. Franz, Phys. Rev. Lett. 111, 206802 (2013).
[14] F. Pientka, L.I. Glazman, F. von Oppen, Phys. Rev. B 88, 155420 (2013).
[15] S. Nadj-Perge, I.K. Drozdov, J. Li, H. Chen, S. Jeon, J. Seo, A.H. MacDonald, B.A. Bernevig, A. Yazdani, Science 346, 602 (2014).
[16] R. Pawlak, M. Kisiel, J. Klinovaja, T. Meier, S. Kawai, T. Glatzel, D. Loss, E. Meyer, Quantum Inf. 2, 16035 (2016).
[17] S. Jeon, Y. Xie, J. Li, Z. Wang, B.A. Bernevig, A. Yazdani, Science 358, 772 (2017).
[18] M. Ruby, B.W. Heinrich, Y. Peng, F. von Oppen, K.J. Franke, Nano Lett. 17, 4473 (2017).
[19] P. Marra, M. Nitta, Phys. Rev. B 100, 220502 (2019).
[20] V. Mourik, K. Zuo, S. M. Frolov, S. R. Plissard, E. P. A. M. Bakkers, and L. P. , Science 336, 1003 (2012).
[21] S. M. Albrecht, A. Higginbotham, M. Madsen, F. Kuemmeth, T. S. Jespersen, J. Nygard, P. Krogstrup, and C. Marcus, Nature (London) 531, 206 (2016).
[22] M.-T. Deng, S. Vaitiekėnas, E. B. Hansen, J. Danon, M. Leijnse, K. Flensberg, J. Nygard, P. Krogstrup, and C. M. Marcus, Science 354, 1557 (2016).
[23] M.-T. Deng, S. Vaitiekėnas, E. Prada, P. San-Jose, J. Nygard, P. Krogstrup, R. Aguado, and C. M. Marcus, Phys. Rev. B 98, 085125 (2018).
[24] E. Prada, R. Aguado, and P. S-Jose, Phys. Rev. B 96, 085418 (2017).
[25] L. Fu and C. L. Kane, Phys. Rev. Lett. 100, 096407 (2008).
[26] S. Zhu, L. Kong, L. Cao, H. Chen, M. Papaj, S. Du, Y. Xing, W. Liu, D. Wang, C. Shen, F. Yang, J. Schneeloch, R. Zhong, G. Gu, L. Fu, Y.-Y. Zhang, H. Ding, and H.-J. Gao, Science 367, 189 (2020).
[27] U. Fano, Phys. Rev. 124, 1866 (1961).
[28] A. E. Miroshnichenko, S. Flach, and Y. S. Kivshar, Rev. Mod. Phys. 82, 2257 (2010).
[29] A. Schuray, L. Weithofer, and P. Recher, Phys. Rev. B 96, 085417 (2017).
[30] A. Ueda, T. Yokoyama, Phys. Rev. B 90, 081405 (2014).
[31] J.-J. Xia, S.-Q. Duan, W. Zhang, Nanoscale Res. Lett. 10, 223 (2015).
[32] C. Jiang, Y.-S. Zheng, Solid State Commun. 212, 14 (2015).
[33] Q.-B. Zeng, S. Chen, L. You, R. Lu, Front. Phys. 12, 127302 (2016).
[34] Y. Xiong, Chin. Phys. Lett. 33, 057402 (2016).
[35] J. Baranski, A. Kobia lka, T. Domanski, J. Phys. Condens. Matter 29, 075603 (2016).
[36] X.-Q. Wang, S.-F. Zhang, C. Jiang, G.-Y. Yi, W.-J. Gong, Physica E 104, 1 (2018).
[37] J. P. R.-Andrade, D. Zambrano, and P. A. Orellana, Analen Der Physic, 531, 1800498 (2019).
[38] L.S. Ricco, V.L. Campo, I.A. Shelykh, and A.C. Seridonio, Phys. Rev. B 98, 075142 (2018).
[39] H.Lu, R. Lu, and B.-f. Zhu, Phys. Rev. B 71, 235320 (2005).
[40] Y. Marques, W. N. Mizobata, R. S. Oliveira, M. de Souza, M. S. Figueira, I. A. Shelykh, and A. C. Seridonio, Scientific Reports 9, 8452 (2019).
[41] Y. Marques, A. E. Obispo, L. S. Ricco, M. de Souza, I. A. Shelykh, and A. C. Seridonio, Phys. Rev. B 96, 041112(R) (2017).
[42] D. E. Liu and H. U. Baranger, Phys. Rev. B 84, 201308 (2011).
[43] E. Vernek, P. H. Penteado, A. C. Seridonio, and J. C. Egues, Phys. Rev. B 89, 165314 (2014).
[44] L. S. Ricco, F. A. Dessotti, I. A. Shelykh, M. S. Figueira, and A. C. Seridonio, Scientific Reports 8, 2790 (2018).
[45] P. W. Anderson, Phys. Rev. 124, 41 (1961).
[46] H. Bruus and K. Flensberg, Many-Body Quantum Theory in Condensed Matter Physics, An Introduction (Oxford University Press, 2012).